which predict that for the transition $H_2(X^1\Sigma_g^+) \rightarrow H_2^+(X^2\Sigma_g^+) + e$, the maximum population of H_2^+ ions is in the $v' = 2$ state.

The influence of the nature of the target atom or molecule is also of interest. Figure 2(a) shows a spectrum taken with an H_2 target. The phenomena are identical to those observed in the $H_2^+ + Kr$ case with two exceptions. First, the relative cross section for superelastic scattering is approximately $\frac{1}{5}$ that for Kr, and so the energy-change spectrum is somewhat weaker in this case. Second, the inelastic spectrum shows the expected strong inelastic peak corresponding to the $v' = 0 \rightarrow v' = 1$ transition in the H_2 target. Figure 2(b) shows a spectrum taken with H^+ projectile ions of nearly the same velocity. As expected, this spectrum shows only the inelastic process corresponding to the $v' = 0 \rightarrow v' = 1$ transition of H_2.

As we have previously shown,[2] the apparent cross sections for the $\Delta v' = \pm 1, \pm 2, \pm 3$ transitions can be obtained directly from the spectrum. For the $H_2^+ + Kr$ superelastic system at 500 eV H_2^+ kinetic energy, we obtain the following: $\sigma(\Delta v' = -1) = 1.08$ Å^2, $\sigma(\Delta v' = -2) = 0.22$ Å^2, $\sigma(\Delta v' = -3) = 0.047$ Å^2. Similarly, for the $H_2^+ + H_2$ superelastic system at 600 eV kinetic energy, we have the following: $\sigma(\Delta v' = -1) = 0.23$ Å^2, $\sigma(\Delta v' = -2) = 0.081$ Å^2, and $\sigma(\Delta v' = -3) = 0.025$ Å^2. Similar studies with He, Ne, and Ar target atoms clearly show a strong increase of the cross sections with increasing atomic number of the target atom. The relative cross sections for superelastic scattering decrease slowly with increasing kinetic energy, being largest in the 100–500-eV region. It is interesting to note that superelastic collision cross sections for the conversion of vibrational to translational energy are comparable in magnitude and energy dependence to the cross sections for the inverse inelastic process of direct vibrational excitation.

Further measurement in the H_2^+ projectile energy range 100–1500 eV with He, Ne, Ar, Kr, Xe, and H_2 targets are in progress and complete results will be reported later.

*Work supported by a grant from the National Science Foundation.

[1]J. H. Moore, Jr., and J. P. Doering, Phys. Rev. Lett. 23, 564 (1969).

[2]F. A. Herrero and J. P. Doering, Phys. Rev. A 5, 702 (1972).

[3]T. E. Sharp, Lockheed Palo Alto Research Laboratory Report No. LMSC5-10-59-9 (unpublished).

[4]G. H. Dunn, J. Chem. Phys. 44, 2592 (1966).

[5]J. Berkowitz, H. Ehrhardt, and T. Tekaat, Z. Phys. 200, 69 (1967).

[6]R. Spohr and E. von Puttkamer, Z. Naturforsch. 22a, 705 (1967).

Lifetime of the 2S State of He^+†

M. H. Prior
Lawrence Berkeley Laboratory, Berkeley, California 94720
(Received 26 June 1972)

The lifetime of the 2S state of He^+ has been measured by counting decay photons versus time from an ensemble of excited He^+ ions stored in an electromagnetic trap of the Penning type. The result is $\tau_{2S} = 1.922(82)$ msec. This is in agreement with the theoretical value of 1.899 msec. The agreement between theory and experiment implies a new upper limit on the amount of parity impurity in the 2S wave function.

Pioneering experiments[1] have established conclusively that the radiative decay 2S to 1S in He^+ proceeds via spontaneous two-photon emission. This is in strict accord with theory[2] which forbids single-photon electric dipole ($E1$) radiation by parity conservation, and predicts a single-photon magnetic dipole ($M1$) rate $\approx 5\times10^{-6}$ times smaller than that for emission of two $E1$ photons. Recently, Marrus and Schmieder have reported[3] measurements of the 2S lifetime, τ_{2S}, in hydrogenlike Ar^{+17} and S^{+15} by a beam-foil time-of-flight technique. However, except for the establishment of lower limits in H^4 and He^+,[5] an experimental value for τ_{2S} in a low-Z ion has not been reported.

This Letter describes work carried out to determine τ_{2S} in He^+. The results are in agreement with the theoretical value[6] of 1.899 msec and lead to a new upper limit on the amount of parity impurity in the 2S-state wave function in He^+.

The 2S state lies 40.8 above the He^+ 1S ground

state, hence the two photons emitted must have energies such that $h\nu_1 + h\nu_2 = 40.8$ eV. The single-photon distribution with wavelength is then a continuous one with a short-wavelength cutoff at $\lambda_{min} = 304$ Å and extending to infinite wavelength. The distribution rises rapidly from λ_{min} to a peak at ≈ 350 Å after which the intensity falls off roughly as $\exp[-(\lambda - 350)/430]$.

The method used to measure τ_{2S} is basically the same as that used[7] to measure the lifetime of the $n=2$ $^1S_0$ state in Li^+. A quantity ($\approx 10^2$) of He^+ $2S$ ions are created by pulsed electron impact on He gas ($p \approx 10^{-7}$ Torr) at time $t=0$. The ions are confined inside an ion trap for a period of several lifetimes (typically 8 msec). During this storage time, single decay photons are detected by windowless electron multipliers and the resulting pulses are stored versus time in 100 channels of a multichannel scalar (80 μsec/channel). At the end of the storage period, all ions are dumped from the trap and a new cycle is begun. Many fill-store-dump cycles are repeated until a decay curve is built up which has a sufficiently small statistical error to allow determination of a value for τ_{2S}. (This may take from 15 min to 2 h depending on the experimental condition.)

An important consideration in any experiment to measure the lifetime of He^+ $2S$ is the nearness of the $2P_{1/2}$ state, the separation being the Lamb shift $S \approx 14.045$ GHz. The radiative lifetime of the $2P_{1/2}$ state is $\tau = 10^{-10}$ sec. Hence, any perturbation which mixes $2S$ and $2P_{1/2}$ can drastically affect (quench) the $2S$ state. In particular, an electric field E will cause mixing via the Stark effect, and yield an effective lifetime τ' given by

$$\tau' = \tau_{2S}\tau_P/(\tau_P + b^2\tau_{2S}),$$

where

$$b^2 = \frac{(4\pi\tau_P)^2|M|^2}{h^2 + (4\pi\tau_P hS)^2} \quad \text{and} \quad M = \sqrt{3}\, eEa_0/Z .$$

For He^+ $b = 7.87\times10^{-5}E$(V/cm) and, hence, electric fields less than 1.0 V/cm are required if τ' is to be within 10% of the field-free value τ_{2S}. Magnetic fields will also cause quenching via the motional electric field $\vec{E}_m = (\vec{v}/c)\times\vec{B}$; e.g., for $v = 2.5\times10^5$ cm/sec, $E_m < 1.0$ V/cm for $B < 400$ G. For these reasons the ion trap operates with rather low magnetic (≈ 50 G) and electric fields (≈ 0.1 V/cm). Weak fields will not confine ions to small volumes, which explains the large size of this ion trap ($\approx 2\times10^4$ cm^3) compared to a similar trap (≈ 10 cm^3) used in the work[7] on Li^+.

Figure 1 shows the ion trap and photon detectors. The ion trap is a closed cylinder (radius ≈ 15 cm, length ≈ 30 cm) whose ends are maintained at a positive potential with respect to the body; potentials used range from 0.5 to 3 V. A magnetic field from 40 to 65 G is applied coaxial with the cylinder by means of coils external to the vacuum enclosure. The electrostatic field confines ion motion along the magnetic field, while the magnetic field limits motion perpendicular to the trap axis.

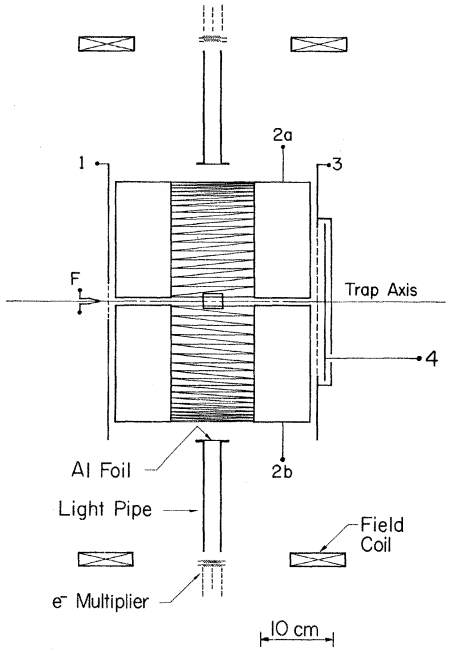

FIG. 1. Sketch of the ion trap and photon detectors. The magnetic field is along the trap axis. The half cylinders $2a$ and $2b$ are maintained negative with respect to electrodes 1 and 3 during the storage period. The hot filament F is pulsed negative to accelerate electrons into the trap for creation of the He ions. The zigzag pattern is a web of thin copper wires to give high transparency for the decay photons, while maintaining the cylindrical electrode geometry. The rectangular shape in the center of the figure represents the end of the microwave horn located outside the cylinder. Power radiated from this horn drives the $2S$-$2P_{1/2}$ transition.

The trap is constructed primarily from oxygen-free high-conductivity copper, stainless steel, and alumina insulators, and the vacuum enclosure is entirely of stainless steel. After bake-out, pressures of $<2\times10^{-9}$ Torr were achieved, and during data collection the background gas pressure is always less than 5×10^{-8} Torr. Helium gas is admitted to the chamber containing the trap via a micrometer needle valve which allows varying the He pressure to study the effects of collisional quenching on the $2S$ decay rate.

Helium ions are created in the trap by impact from an electron pulse accelerated along the axis of the magnetic field. Typically the electron pulse is 100 μA, lasts 0.75 msec, and has an energy of 225 eV. At a helium pressure of 1.7×10^{-7} Torr this yields about 2×10^{5} ions, of which approximately 200 can be expected to be in the $2S$ metastable state. At the end of a storage period the trap potentials are altered so that ions are dumped onto a collecting plate (electrode 4 in Fig. 1); this allows monitoring of the number of stored ions via the size of the resulting positive-current pulse. The electron pulse also appears on this electrode during the trap fill time.

As is indicated in Fig. 1, the cylindrical portion of the trap is made up of two half cylinders $2a$ and $2b$; this allows application of an alternating potential between them (while maintaining a common dc potential) which can excite resonant motion of the stored ions at their cyclotron frequency. At resonance the ions gain energy from the ac field until they strike the electrodes or chamber walls; thus one observes a drop in the ion-dump pulse amplitude when the applied frequency is in resonance. In addition to the cyclotron resonance, one observes resonance at the frequency of motion along the trap axis (z motion) and at the magnetron frequency (frequency of drift of the cyclotron orbit center about the trap axis).

The photon detectors are two EMI 9642/2 eighteen-stage CuBe venetian-blind electron multipliers. To prevent metastable helium atoms ($2\,^3S_1$ and $2\,^1S_0$) from reaching the multipliers, their view of the storage volume is covered by aluminum foils 18 mm in diameter and 800 Å thick. The foils have a transmission varying between 10% and 70% over the region 200 to 700 Å. The Al-foil–CuBe-multiplier combination responds to $\approx 2\%$ of the radiation over the range 300 to 500 Å which strikes the Al foil. The two light pipes are Pyrex tubes coated internally with a 1000 Å thickness of gold; they enhance the count rate by about a factor of 4 over the case with no light pipes.

To establish that the observed decay is that from He^+ $2S$, microwave power (≈ 150 mW) at the Lamb-shift frequency (14.045 GHz) is broadcast into the trap volume via a wave-guide horn. This converts a large fraction (more than 80%) of the $2S$ ions to the $2P_{1/2}$ state from which they immediately decay, destroying the $2S$ decay curve. Measurement of the quenching versus microwave frequency yielded a Lamb-shift resonance curve.

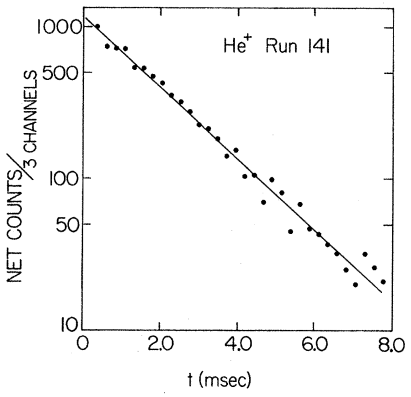

FIG. 2. Representative He^+ $2S$ decay curve. The line is a computer fit which gave $\tau = 1.866$ msec. The final result is a corrected mean value derived from 19 such runs.

The microwave power is generated by a Varian X-12 klystron and may be on-off modulated via a p-i-n-diode switch under control of the data-collection logic system.

One typical data cycle consists of the following sequence: a 0.75-msec fill period during which time the electron pulse is on, a delay period of 0.8 msec during which the microwave power may or may not be applied, a storage period of 8 msec during which counts from the multipliers are accumulated versus time in 100 channels of the memory unit, and a 75-μsec ion dump period. Data are stored in two separate 100-channel blocks of the memory unit corresponding to whether or not microwave power is on or off during the delay period. Usually the microwave power is switched on or off every 5000 data cycles. The time base for the system is derived from a 100-kHz crystal oscillator.

Figure 2 shows a decay curve representative of those used to determine τ_{2S}. The data are the difference between counts accumulated with microwave power on and off. Each point is the sum of three 80-μsec channels. The ratio of total counts with power off to power on was about 6:1. About 90 min were required to collect these data. The straight line through the points is the least-squares–fitted exponential decay curve which yielded $\tau = 1.866$ msec.

The final result is based on a total of 19 runs similar to that shown in Fig. 2. During these runs the trapping potential was 0.9 V, the magnetic field was 42.5 G, and the He pressure was $\approx 1.7\times10^{-7}$ Torr. The mean value of the 19-run set is 1.864 msec with a standard deviation for a single run from the mean of 0.079 msec. The

mean value must be corrected slightly to allow for collisional and field quenching.

The effect of collisional quenching was studied by varying the He pressure up to a maximum of $\approx 5.5\times10^{-6}$ Torr. The resulting plot of τ^{-1} versus pressure yielded a positive correction of 0.035 msec to be added to the mean of the 19 runs.

The effect of quenching by the trap fields is taken into account by considering a hypothetical worst case. The maximum kinetic energy of a trapped ion was ≈ 1.0 eV (the trapping potential plus the maximum recoil energy). This corresponds to a velocity of 7×10^5 cm/sec. In a 42.5-G magnetic field this yields as a maximum motional electric field $E_m = 0.28$ V/cm. A good estimate of the maximum static electric field in the trap is given by

$$E_s = (M/q)A_z(2\pi f_z)^2 ,$$

where M is the ion mass, q is the ion charge, and A_z and f_z are the amplitude and frequency of the z motion. For He^+ ions with $A_z = 15$ cm, and the observed $f_z = 12.2$ kHz, one obtains $E_s = 0.37$ V/cm. Combining E_s and E_m vectorially yields $E = 0.46$ V/cm as a worst-case estimate of the maximum electric field seen by an ion in the trap. This would produce a quenching effect of 2.5% on the $2S$ lifetime. To account for field quenching then, we assume a positive correction of 1.25% (0.023 msec) and include the same amount in computing the uncertainty in the result.

The final result is then $\tau_{2S} = 1.922(82)$ msec. The uncertainty is the quadrature sum of the 0.079-msec standard deviation of the 19-run distribution and the 0.023-msec uncertainty in the field-quench correction.

The agreement between experiment and theory implies a limit on the amount of $2P_{1/2}$ state that may be mixed with $2S$ by a hypothetical parity-nonconserving neutral weak current and/or electromagnetic interaction.[8-10] Thus, if the wave function is written $\psi(2S) = \varphi(2S) + \epsilon\varphi(2P_{1/2})$ with the φ's Schrodinger wave functions, the uncertainty in the result quoted here for τ_{2S} implies $|\epsilon| < 4.7\times10^{-5}$. This is an improvement by a factor of 10 over a previous limit based on τ_{2S} in Ar^{+17} (Ref. 3).

†Work supported in part by the U. S. Atomic Energy Commission.

[1]An excellent summary is given by R. Novick, in *Physics of the One- and Two-Electron Atoms*, edited by F. Bopp and H. Kleinpoppen (North-Holland, Amsterdam, 1969), p. 296 ff.

[2]H. A. Bethe and E. E. Salpeter, *Quantum Mechanics of One- and Two-Electron Atoms* (Academic, New York, 1957), Chap. 4, p. 285.

[3]R. Marrus and R. W. Schmieder, Phys. Rev. A 5, 1160 (1972).

[4]W. L. Fite, R. T. Brackman, D. G. Hummer, and R. F. Stebbings, Phys. Rev. 116, 363 (1959).

[5]E. Commins, L. Gampel, M. Lipeles, R. Novick, and S. Schultz, Bull. Amer. Phys. Soc. 7, 258 (1962); M. Lipeles, R. Novick, and N. Tolk, Phys. Rev. Lett. 15, 690 (1965).

[6]J. Shapiro and G. Breit, Phys. Rev. 113, 179 (1959); S. Klarsfeld, Phys. Lett. 30A, 382 (1969).

[7]M. H. Prior and H. A. Shugart, Phys. Rev. Lett. 27, 902 (1971).

[8]Ya. B. Zel'dovich and A. M. Perelomov, Zh. Eksp. Teor. Fiz. 39, 1115 (1960) [Sov. Phys. JETP 12, 777 (1961)].

[9]R. A. Carhart, Phys. Rev. 132, 2337 (1963); J. Bernstein, M. Ruderman, and G. Feinberg, Phys. Rev. 132, 1227 (1963).

[10]B. Sakitt and G. Feinberg, Phys. Rev. 151, 1341 (1966).